Automated Decellularization of the Rodent Epigastric Free Flap: A Comparison of Sodium Dodecyl Sulfate–Based Protocols

Fuat Baris Bengur, MD[1,*] Lei Chen, MD[1,*] Benjamin K. Schilling, PhD[1,2] Chiaki Komatsu, MD[1] Grace M. Figlioli[1,2] Kacey G. Marra, PhD[1,2,3] Lauren E. Kokai, PhD[1,3] Mario G. Solari, MD[1,3]

[1] Department of Plastic Surgery, University of Pittsburgh, Pittsburgh, Pennsylvania
[2] Department of Bioengineering, University of Pittsburgh, Pittsburgh, Pennsylvania
[3] McGowan Institute for Regenerative Medicine, University of Pittsburgh, Pittsburgh, Pennsylvania

Address for correspondence Mario G. Solari, MD, Division of Plastic Surgery and Otolaryngology, Department of Plastic Surgery, University of Pittsburgh, 3550 Terrace Street, 6B Scaife Hall, Pittsburgh, PA 15261 (e-mail: solarimg@upmc.edu).

J Reconstr Microsurg 2023;39:493–501.

Abstract

Background Free tissue transfer to cover complex wounds with exposed critical structures results in donor-site morbidity. Perfusion decellularization and recellularization of vascularized composite tissues is an active area of research to fabricate complex constructs without a donor site. Sodium dodecyl sulfate (SDS)-based protocols remain the predominant choice for decellularization despite the deleterious effects on tissue ultrastructure and capillary networks. We aimed to develop an automated decellularization process and compare different SDS perfusion times to optimize the protocol.

Methods A three-dimensional-printed closed-system bioreactor capable of continuously perfusing fluid through the vasculature was used for decellularization. The artery and vein of rat epigastric fasciocutaneous free flaps were cannulated and connected to the bioreactor. Protocols had varying durations of 1% SDS solution (3, 5, and 10 days) followed by 1 day of 1% Triton X-100 and 1 day of 1x phosphate-buffered saline. The residual DNA was quantified. Microarchitecture of the constructs was assessed with histology, and the vascular network was visualized for qualitative assessment.

Results The structural integrity and the microarchitecture of the extracellular matrix was preserved in the 3- and 5-day SDS perfusion groups; however, the subcutaneous tissue of the 10-day protocol lost its structure. Collagen and elastin structures of the pedicle vessels were not compromised by the decellularization process. Five-day SDS exposure group had the least residual DNA content ($p < 0.001$). Across all protocols, skin consistently had twice as much residual DNA over the subcutaneous tissues.

Conclusion A compact and integrated bioreactor can automate decellularization of free flaps to bioengineer regenerative constructs for future use in reconstruction of complex defects. A decellularization protocol with 5 days of 1% SDS exposure was the most successful to keep the residual DNA content at a minimum while preserving the structural integrity of the tissues.

Keywords
- decellularization
- vascularized tissue engineering
- fasciocutaneous free flap
- extracellular matrix
- allograft

* *These authors contributed equally.*

received
May 19, 2022
accepted after revision
October 31, 2022
article published online
December 30, 2022

Thieme Medical Publishers, Inc.,
333 Seventh Avenue, 18th Floor,
New York, NY 10001, USA

DOI https://doi.org/10.1055/s-0042-1760110.
ISSN 0743-684X.

Complex wounds with exposed critical structures after trauma or cancer ablation, such as bone, tendon, blood vessels, nerve, or hardware, require reconstruction with vascularized tissues. Local and regional tissue flap reconstructions may be unavailable in extensive injuries and larger defects.[1] Therefore, autologous free tissue transfer is often the preferred method for complex wound reconstruction.[2] Composite tissues can be used to fill large defects, recreate damaged contours, or provide reliable coverage over exposed structures. However, free flap surgery is an expensive and lengthy operation that results in donor-site morbidity, such as scarring, pain, and loss of function.[3,4]

The current pinnacle of free flap surgery is vascularized composite allotransplantation, such as hand and face transplantation. Allotransplantation has the advantage of eliminating donor-site morbidity, but also carries the risks of infection, neoplasia, and immunological reaction in the recipient.[5,6] Therefore, engineered vascularized tissue flaps offer an ideal and clinically viable alternative. Successful use of such constructs without immunosuppression requires thorough removal of host cells through decellularization. Decellularized scaffolds can then be recellularized with recipient-derived or immunoprivileged cells to recreate the vasculature and microarchitecture. Finally, the engineered free flap can be transferred back to a patient, providing coverage of the defect without donor-site morbidity.

The ability to decellularize and eventually recellularize solid organs and vascularized composite tissues are active areas of research toward fabricating off-the-shelf vascularized constructs.[7–9] A recellularized solid organ, facial tissue, or limb allograft presents with significant challenges due to metabolic function and complexities of the tissues. A fasciocutaneous free flap is a much simpler construct and has broader clinical indications compared with limb and facial tissue allografts. The initial step to achieve the goal of an off-the-shelf free flap is successful decellularization that preserves the composition and structure of the extracellular matrix (ECM). The minimal criteria to demonstrate the success of decellularization have been defined as DNA content below 50 ng/mg and lack of visible nuclear material.[10] Additionally, mass transfer of oxygen is the rate-limiting factor for cell survival in tissue-engineered constructs.[11] In native tissue, cells are typically within 100 to 200 µm of the nearest capillary to allow for sufficient influx of oxygen and nutrients and efflux of carbon dioxide and cellular waste.[12] As such, to engineer a composite allograft more than 200 µm thick, an internal vascular network is required to prevent core necrosis. Therefore, approaches using the tissue's intrinsic network by means of perfusion decellularization have shown exceptional promise in whole organ engineering.[13–18] However, these approaches have seen minimal crossover into the microsurgical field with composite tissues.[19–23]

Sodium dodecyl sulfate (SDS) is the predominant choice of detergent for decellularization protocols.[18,24] However, SDS also has deleterious effects on the ultrastructure and capillary network of the scaffold.[25] The optimal duration of exposure has not been determined for vascularized composite soft tissue decellularization, which is a critical step to determine the success of future recellularization approaches. Additionally, current protocols for tissue decellularization can be time intensive and require overhead in terms of equipment. Automation of the decellularization process can decrease hands-on time and increase repeatability. However, automation systems are often developed for a specific tissue and typically include several unwieldy components that restrict easy operation.[26] To facilitate this process, we have previously designed and fabricated a functional and reproducible tissue infusion and perfusion bioreactor, using three-dimensional-printed parts.[27] In this study, we aimed to optimize the SDS exposure protocol for automated decellularization of fasciocutaneous rodent soft tissue flaps by comparing different SDS perfusion times to find the balance between decellularization and scaffold preservation.

Methods

Fasciocutaneous Free Flap Harvest and Preparation

The Institutional Animal Care and Use Committee of the University of Pittsburgh approved the animal protocol used in this study. Sprague Dawley rats (6–8 weeks, Charles River Laboratories, Wilmington, MA) were anesthetized using 2.5% isoflurane in 100% oxygen, followed by an intraperitoneal injection of ketamine (Ketaset, 50 mg/kg), xylazine (AnaSed, 2.5 mg/kg), and acepromazine (AceproJect, 1.25 mg/kg) immediately prior to flap harvest. In the supine position, the epigastric flap harvest site was[28] shaved and prepared with 70% alcohol, and two 3×3 cm flaps were marked (►**Fig. 1A**). A full-thickness incision, including the skin and subcutaneous tissues above the facia, was made in the abdominal wall. The superficial inferior epigastric vessels were exposed and preserved. The femoral vessels were divided distal to the origin of the superficial inferior epigastric vessels. The flap was then raised in a superior-to-inferior

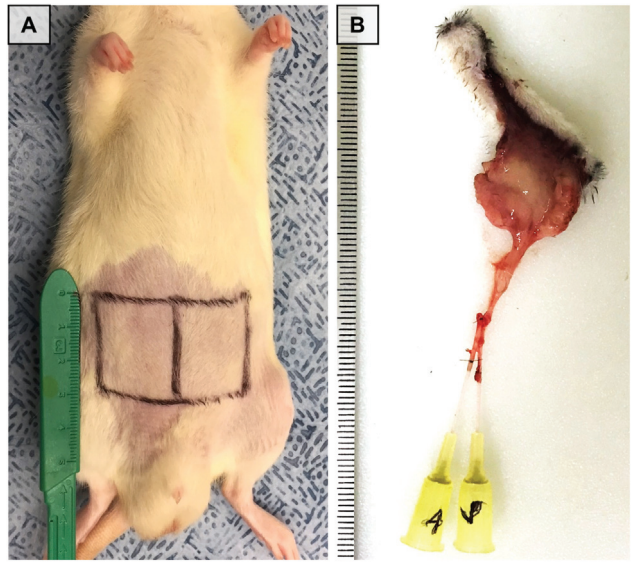

Fig. 1 (A) Design of the 3×3 cm epigastric fasciocutaneous free flap, harvested from a rat, shown oriented in the supine position. (B) The free flap after harvest and cannulation of the femoral artery and vein with 24G catheters.

direction. The femoral vessels were ligated and divided. 24G catheters were inserted into femoral artery and vein, and secured with 7–0 Nylon sutures (Microsurgery Instruments, Bellaire, TX) (►**Fig. 1B**). The flap was immediately flushed with heparinized saline (10 U/mL). Animals were euthanized following procurement of the flaps.

Perfusion Decellularization

A previously designed and fabricated tissue infusion and perfusion bioreactor composed of 3D printed and commercially available components including two peristaltic pumps, two three-way valves, and a chamber was used for all decellularization protocols (►**Fig. 2A–C**).[27] An automation function was integrated to user-customizable software (LabVIEW, National Instruments, Austin, TX), which is able to specify fluid flow rates and define valve open/close protocols, enabling selection of solutions over the course of the process. The flow characteristics of the bioreactor were previously described.[27]

The perfusion system was primed with heparinized saline (10 U/mL). The cannulated flap was connected to the perfusion bioreactor through its artery (inflow) and vein (outflow) (►**Fig. 2D, E**). The flap was placed on a meshed platform, which allowed for drainage of the exudate and the venous outflow into a waste reservoir. The peristaltic pump speed was initially set at the lowest speed and the decellularization procedure was initiated by perfusing through the arterial catheter with the following solutions: (1) 10 units/mL heparinized saline for 1 hour, (2) varying durations of 1% SDS, (3) 1% Triton X-100 for 24 hours, and (4) 1x phosphate buffered saline for 24 hours (all reagents: MilliporeSigma, Burlington, MA). The flaps were divided into three groups with 3, 5, and 10 days of perfusion with 1% SDS (►**Fig. 3**). The perfusion pressure was kept below 120 mm Hg.

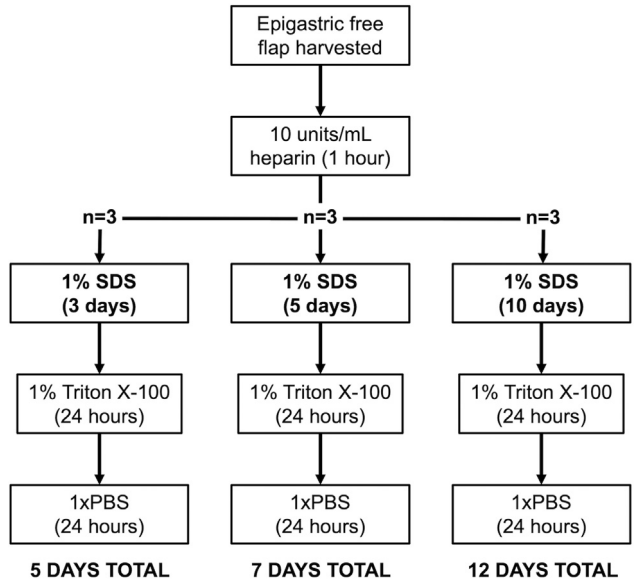

Fig. 3 Flow diagram of the decellularization processes with varying exposure times of perfused SDS. PBS, phosphate-buffered saline; SDS, sodium dodecyl sulfate.

Macroscopic Evaluation

After the decellularization process, flaps were visually inspected to assess macrostructural integrity and removal of cellular components by changes in the tissue color.

Histomorphometric Analysis

Upon completion of the decellularization protocol, a 10% formalin solution was infused through the arterial catheter using the bioreactor for 30 minutes. Specimens were then removed from the bioreactor and fully submerged in a 10% formalin solution at 4°C for 3 days. After fixation, all samples were divided into four sections as (1) distal, (2) middle, (3)

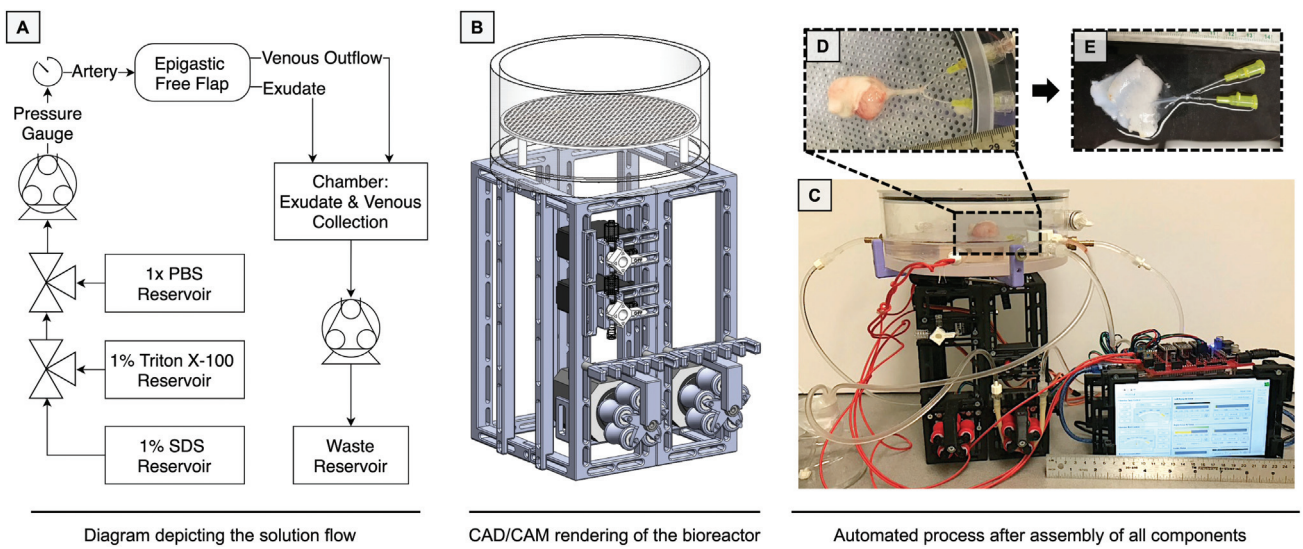

Fig. 2 (A) Diagram depicting solution flow into and out of the free flap via the perfusion bioreactor. (B) CAD/CAM rendering of the perfusion bioreactor used for free flap decellularization. (C) The bioreactor after printing and assembly of all components. (D) The fasciocutaneous free flap connected to the bioreactor with arterial and venous catheters. (E) The decellularized fasciocutaneous free flap. CAD, computer-aided design; CAM, computer-aided manufacturing; PBS, phosphate-buffered saline; SDS, sodium dodecyl sulfate.

proximal, and (4) pedicle and then embedded in paraffin. Specimens were sectioned serially along the horizontal axis (10-µm thickness), using a low temperature water bath. All sections were stained with hematoxylin and eosin (H&E) and Masson's trichrome to visualize the residual nuclear material and assess structural changes in the ECM and collagen fibers. Additionally, the pedicles were also stained with Verhoeff–Van Gieson (VVG) stain for assessing the integrity of the vasculature. All staining was performed by the Histology Core Facility, McGowan Institute for Regenerative Medicine, University of Pittsburgh.

DNA Quantification

Decellularized flaps ($n = 3$/group) were divided into four sections (►**Supplementary Fig. S1**, available in the online version) according to the distance between the most distal aspect of the flap and the entrance of the pedicle to the flap as (1) proximal, (2) proximal–distal, (3) distal–proximal, and (4) distal. AllPrep DNA/RNA/Protein Mini Kit (Qiagen, Germany) was used to extract DNA from the tissues and Quant-iT PicoGreen dsDNA assay kit (P7589, Invitrogen, Waltham, MA) was used to quantify the DNA content. Decellularized tissues were freeze-dried for 24 hours and weighed before tissue homogenization. Then tissues were mixed with 600 µL buffer RLT and homogenized for 30 seconds. Supernatants from the samples were moved to a 96-well plate and diluted Quant-iT PicoGreen dsDNA reagent (1:200) was added into the supernatants. Samples were then measured for fluorescence intensity using Infinite 200 PRO plate reader (Tecan, Switzerland), and the measured DNA quantity was normalized to the initial dry weight of the tissue. Measurements were performed both from the skin and subcutaneous side of the flaps.

Vascular Corrosion Casting

Vascular corrosion casting was performed using Batson's No. 17 corrosion kit (Polysciences, Inc, Warrington, PA). A total of 10 mL base solution A was mixed with 1.5 mg of blue or red pigment, 2.5 mL of catalyst, and 20 drops of promotor. Once the decellularization was completed, catheters were detached from the bioreactor, and the final red solution of 1 mL was immediately injected with a syringe through the arterial catheter for 5 minutes. Once completed, the final blue solution was similarly injected from the venous catheter. The flap was placed on an ice bath for 2 hours, followed by digestion of the surrounding tissue with 25% KOH solution for 24 hours.

Statistical Analysis

All quantitative data are expressed as means ± standard deviations. JMP Pro (Cary, NC) statistical suite was used for all analyses. Comparisons between the groups were performed by repeated measures analysis of variance after verifying normality of residuals by Shapiro–Wilk W test. Significance was established for differences with p-values of less than 0.05.

Results

Macroscopic Evaluation

Decellularization was successfully performed in all three groups with varying protocol durations. Decellularization resulted in a visible color change from a red flesh tone of the subcutaneous tissues to white and partially translucent (►**Fig. 4**). The color change was more prominent in the 10-day SDS exposure group, where certain skin portions of the flap were macerated and disintegrated (►**Supplementary Fig. S2**, available in the online version). All flaps were edematous and increased in size. Arteries and veins of the flaps were visually intact and clearly distinguishable from the surrounding tissues.

Histomorphometric Analysis

In general, staining with H&E and trichrome demonstrated the presence of structural elements such as the ECM and collagen fibers, as well as the absence of nuclear and cellular remnants in the majority of the flap cross-sectional area (►**Fig. 5**). Compared with a nondecellularized flap, cellular

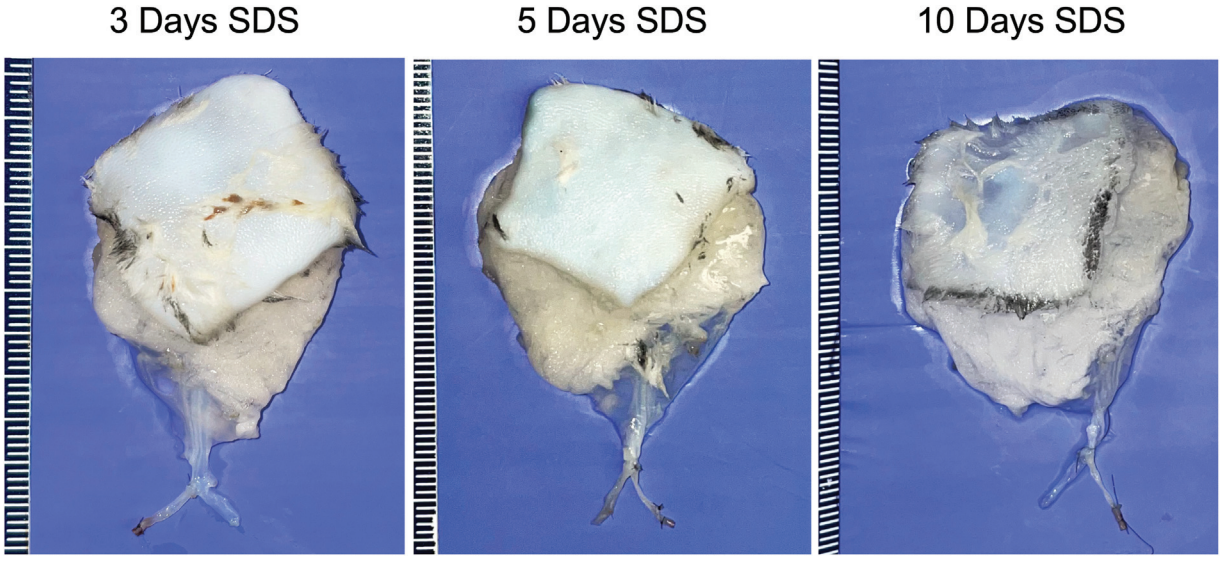

Fig. 4 Resulting appearance of the scaffolds after each decellularization process. Ruler demarcations represent 1 mm. SDS, sodium dodecyl sulfate.

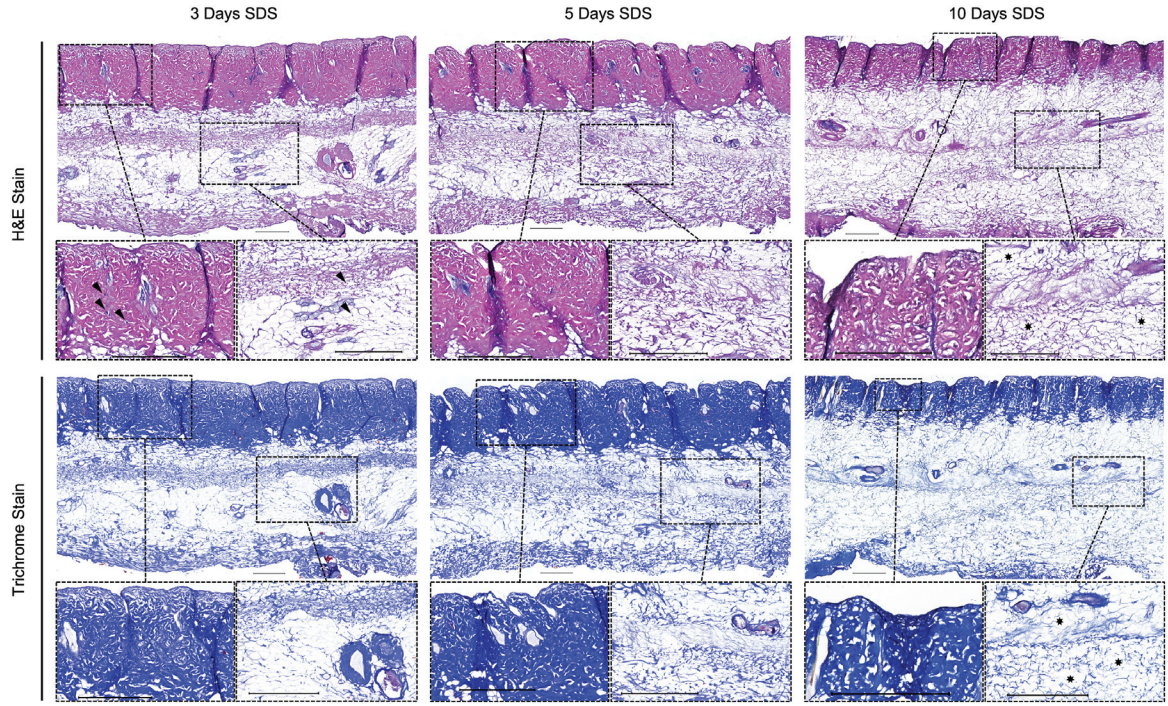

Fig. 5 Cross-sections from the middle region of the flaps after each decellularization protocol are demonstrated with H&E and trichrome staining. Higher magnification views are provided from the skin and subcutaneous compartments of each group. Arrows point out the retained residual nuclear material and stars denote the areas of damaged extracellular matrix. H&E, hematoxylin and eosin; SDS, sodium dodecyl sulfate. Scale bars: 500 μm.

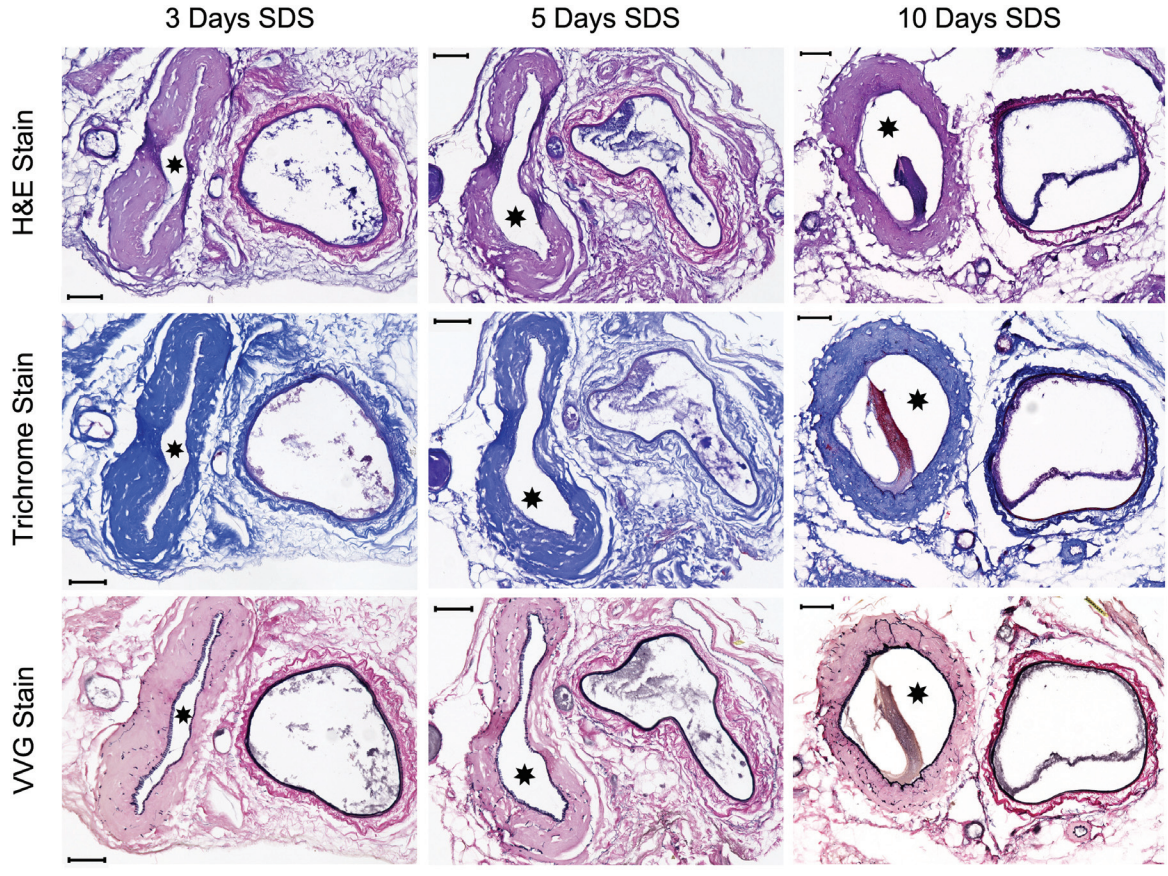

Fig. 6 Cross-sections from the flap pedicles after each decellularization protocol are demonstrated with H&E, trichrome, and VVG staining. Arterial lumens are marked with a star. In all sections, both vessels were preserved with intact collagen and elastin structures. H&E, hematoxylin and eosin; SDS, sodium dodecyl sulfate; VVG, Verhoeff–Van Gieson. Scale bars: 100 μm.

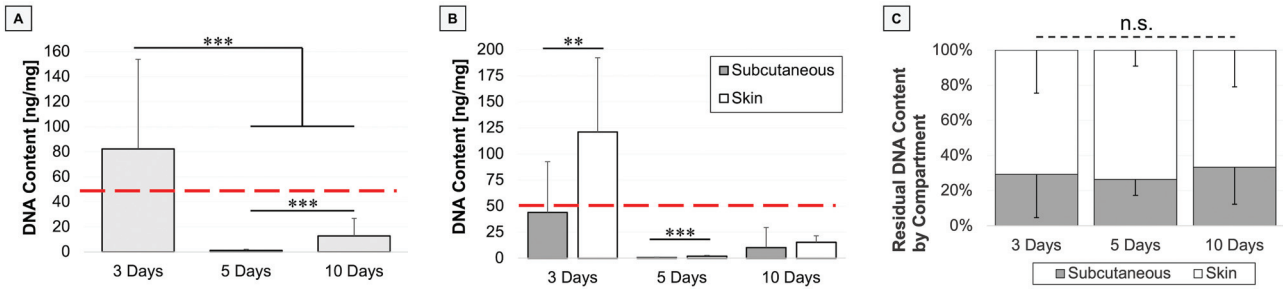

Fig. 7 (A) DNA quantification grouped by SDS perfusion time. (B) DNA quantification grouped by SDS perfusion time and compartment. Dashed lines denote the DNA content threshold of decellularization at 50 ng/mg. (C) DNA content of each compartment normalized to the total DNA in each sample. n.s., not significant; SDS, sodium dodecyl sulfate. $^{**}p < 0.01$ and $^{***}p < 0.001$.

components in the parenchymal tissues such as epithelial cells, fibroblasts, adipocytes, endothelial cells, and smooth muscle cells were not apparent. In the 3-day SDS exposure group, occasional spots of residual nuclei were detectable in H&E staining. Trichrome staining confirmed a substantially diffuse and homogenous retention of the collagen content in all the groups. While the structural integrity and the microarchitecture of the ECM were preserved in the 3- and 5-day SDS exposure groups, the ECM around the subcutaneous tissues of the 10-day protocol lost its definition as well as the major architectural components of the basal membrane. These changes were consistent across all sections of the flaps (►**Supplementary Fig. S3**, available in the online version). Microvascular components, such as the arterioles and capillaries were diffusely present in all the groups, as demonstrated by both stains. For the pedicle vessels in all the groups, trichrome and VVG staining for collagen and elastin structures of vessels were not compromised by the decellularization process (►**Fig. 6**). However, in the 10-day SDS exposure group, structures in the perivascular space lost their definition.

DNA Quantification

For the overall DNA content per milligram of freeze-dried tissue, the 5-day SDS exposure group had the least residual DNA content (1.309 ± 0.807 ng/mg) followed by the 10-day

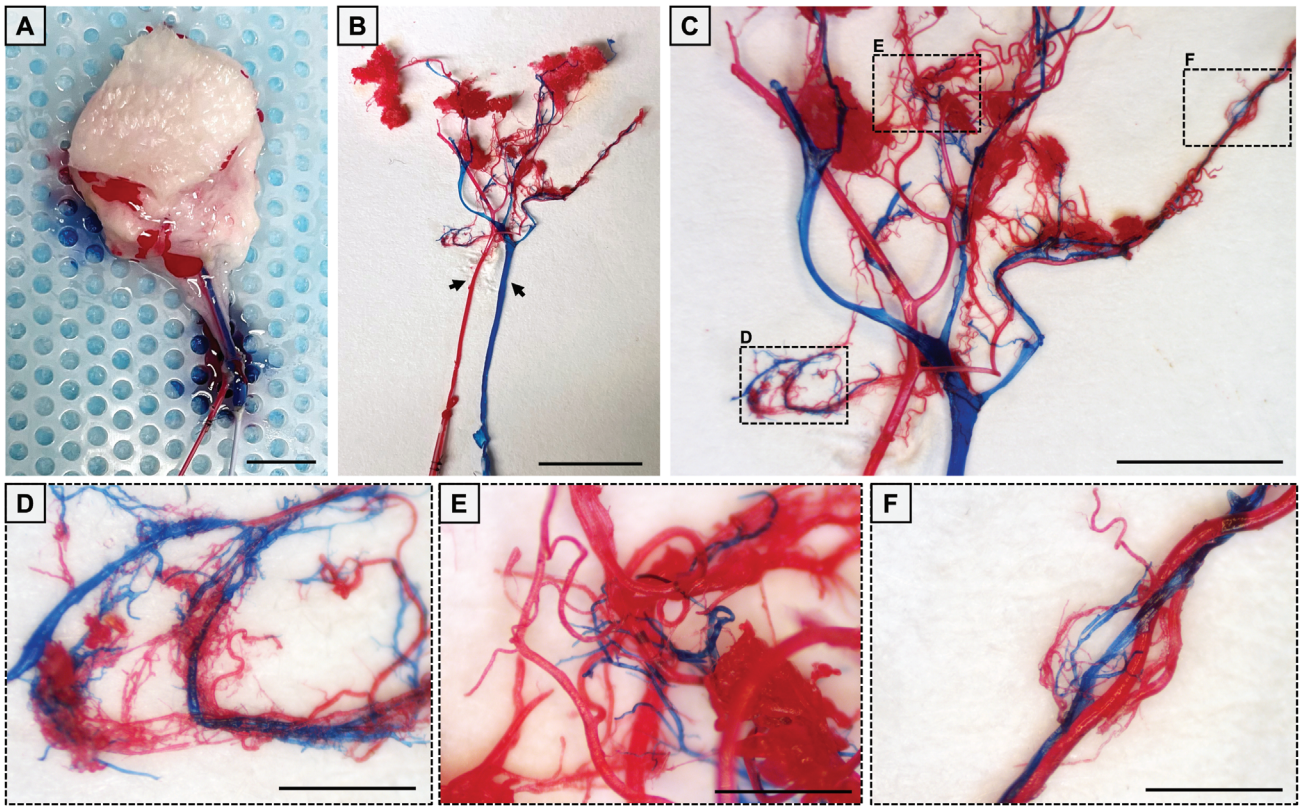

Fig. 8 (A) Corrosion casting of a decellularized flap from the 5-day SDS exposure group. Note that the infused red and blue casting solutions create contrast with the white flap. Scale bar: 1 cm. (B) The cast demonstrating the internal vascular network after digestion of the surrounding tissues. Red represents the arterial network, while blue represents venous. Arrows point out the main pedicle vessels. Scale bar: 1 cm. (C) Magnified view of the cast to demonstrate the fine vessels. Scale bar: 5 mm. (D–F) Higher magnification of the distal vessels and arteriovenous connections. Scale bars: 1 mm. SDS, sodium dodecyl sulfate.

(12.684 ± 14.184 ng/mg) and 3-day (82.387 ± 71.595 ng/mg) groups, $p < 0.001$ (►**Fig. 7A**). When the residual DNA content was analyzed based on the location as skin versus subcutaneous, skin had significantly higher amounts in the 3-day ($p < 0.01$) and 5-day ($p < 0.001$) exposure groups (►**Fig. 7B**). The DNA content ratio of skin over subcutaneous tissues was consistent across all protocols with skin having twice as much residual DNA after each protocol (►**Fig. 7C**). When the DNA content was analyzed for distance from the pedicle, the distal segments of the 3-day SDS exposure group had a significantly higher residual content versus the rest (►**Supplementary Fig. S1**, available in the online version).

Vascular Corrosion Casting

The vascular network in the 5-day SDS exposure group was visualized for qualitative assessment with the infusion of the hardening cast to create contrast against soft tissue (►**Fig. 8A**). Once the surrounding tissue was digested, the remaining cast revealed an intact arterial and venous vascular network (►**Fig. 8B, C**). Small capillaries and arteriovenous anastomoses were visible (►**Fig. 8D–F**).

Discussion

Decellularization of allogeneic vascularized composite soft tissue constructs is the critical initial step in creating a viable, off-the-shelf, allograft-based free flap to be recellularized with either immune-privileged or recipient cells. Despite having abundant evidence for whole organ decellularization, protocols for decellularization of soft tissue flaps are not well defined. A comparative analysis of different exposure durations for the reagents as well as a repeatable protocol is needed to gain better understanding of the balance between successful decellularization and scaffold preservation. In this study, we described a fully automated, repeatable, and affordable protocol for perfusion decellularization of rodent fasciocutaneous free flaps. The decellularized scaffold can then be recellularized using the same bioreactor to gradually re-endothelialize the vasculature and recreate the cellular components.

Preservation of native structures, and particularly the vascular network, has an important role in vascularized tissue engineering.[29] Once damaged, recreation of a functional vasculature remains a hallmark challenge; therefore, developing a system tailored to vasculature preservation is essential.[30–33] The use of a tissue's own vascular network, coupled with shearing fluid forces, is capable of removing whole cells and debris while preserving the vasculature.[34–36] Such a perfusion system also offers unique capabilities for recellularization, introducing cells directly into the scaffold by means of its own vasculature while also controlling the fluid mechanics by which the cells are deposited. Therefore, an ideal perfusion system could run the whole process as a closed circuit from controlled decellularization to adequate recellularization of the scaffold. There have been numerous developments on this particular topic to apply this principle to engineer composite tissues for the reconstruction of complex defects throughout the body.[37] To date, however, these approaches are not easily automated and tend to be piecemealed bioreactor solutions. Our tissue infusion and perfusion bioreactor provides an open-source alternative toward consistent and repeatable decellularization of fasciocutaneous free flaps. As the integration of tissue engineering, the use of perfusion bioreactors, and reconstructive microsurgery continue to evolve, identification of the optimal decellularization protocol will serve as the initial step for development of more complex products. Eventually, these products could cause a paradigm shift in the current practice of management of complex soft tissue defects and mitigate current limitations of free tissue transfer, such as donor-site morbidity.[38,39]

There is not a consensus on the duration of SDS exposure in the literature. For similar perfusion decellularization protocols for vascularized composite tissues, Giatsidis et al successfully utilized a 100-hour (~4 days) protocol for human abdominal panniculectomy tissue.[23] Jank et al applied 10 days of SDS perfusion for fasciocutaneous groin flap in miniature swine with success.[20] Qu et al utilized varying durations as 12, 24, and 72 hours of SDS perfusion combined with agitation for rat fasciocutaneous epigastric free flap and suggested the use of a combined protocol with SDS exposure for 24 hours or longer.[21] Unique in our study, we (1) used fully automated protocols, (2) utilized microvascular casting to demonstrate both arterial and venous systems, and (3) quantified the DNA content in different areas of the flaps to identify changes related to the distance from the main vessel branches. All three protocols in our study achieved gross decellularization after macroscopic evaluation. Histological sections showed that the 3-day SDS exposure protocol had local residues of retained nuclear material and the 10-day protocol had lost its ECM architecture and definition. Additionally, flaps in the 10-day group were more fragile compared with the rest, where the subcutaneous tissues started to disintegrate. Therefore, 3- and 5-day protocols successfully preserved the macro- and microstructure of the tissues.

In the 3-day SDS exposure protocol, the residual DNA content was above the threshold of 50 ng/mg of tissue, yielding an unsuccessful decellularization. The distal portions of the skin in the 3-day group had the highest DNA content compared with any other subsections in other groups. This could indicate that with ex vivo perfusion decellularization, an adequate time is necessary to perfuse the most distal portions of the angiosome that are dependent on perfusion from the choke vessels in vivo. Furthermore, the residual DNA content of the 5-day exposure group was significantly lower than the 10-day group. Although it is not expected for the cells to retain their DNA content with increased duration of detergent exposure, this could be explained by (1) damage caused to the vasculature by increased SDS duration and subsequent SDS retention and (2) the reaction of the SDS with the fluorescence-based assay used for DNA quantification. SDS has been reported to have a dose-dependent effect on the binding of the fluorescent dye, where the 0.01% solution had no effect, while the 0.1% solution completely interfered with the measurements.[40,41] In our study, we used a 1% solution of SDS followed by 2 days

of washing with Triton X-100 and phosphate-buffered saline (PBS) to remove the residual solution. This resulted in successful removal of the SDS from the intact vasculature and accurate measurements of the DNA content for the 3- and 5- day groups. However, it is possible that as the duration increased to 10 days and the vasculature was damaged, SDS was retained within the tissues and was not completely removed with 2 days of washing, therefore, interfering with the fluorescence-based assay. These results can be further confirmed qualitatively by the lack of nuclei with H&E staining in 5- and 10-day groups, which is also another criterion for successful decellularization.[10]

On microscopic evaluation of the pedicle vessels, arteries and veins retained their structure with intact elastin and collagen content. When the corrosion casting was performed, arterial and venous vascular networks were also visualized. One challenge reported in the literature is demonstrating a successful venous outflow from engineered free tissue flaps. A recent systematic review showed 11 studies on engineered vascularized composite allografts that demonstrated preservation of microvasculature to a variable extent.[42] However, only five of these studies attempted transplantation of these constructs, where the majority were terminated with no immediate venous return.[20,43–45] Although this could be primarily explained by the thrombogenicity of the transplanted constructs, the ability to preserve the arterial and venous tracts from the deleterious effects of the decellularization solutions is a crucial step for recellularization approaches.

Our study had several limitations. The perfusion pressure was monitored to be below 120 mm Hg throughout the decellularization process in all the groups. A standard pressure value was not kept constant however, as each flap had varying degrees of intravascular resistance both in between iterations as well as within each flap over the decellularization process. It is possible that damage to the weakest point within the vascular tree, perhaps being the vessels that were cauterized during flap harvest, led to leakage around the flap as observed by fluid collection at the exudate reservoir. Despite seeing both arterial and venous networks, there was some disconnection between both circulations that could lead to a lack of a closed circuit. Aggressive pressure controlling, potentially at subphysiological levels, could be necessary to completely preserve fragile decellularized vessels. Second, the vascular corrosion casting was only performed at the 5-day SDS exposure group to assess patency of the vascular network. This group was chosen after the DNA quantification and histomorphometric analysis as being the optimal protocol. It should be also noted that the patency of the vascular network could improve after recellularization. Third, additional metrics could be used to correlate the trend in residual DNA content, such as gel electrophoresis. Finally, our study was performed in a rodent fasciocutaneous free flap model. It is possible that larger tissues with different components could require varying durations of SDS exposure and different protocols. Nevertheless, the tissue infusion and perfusion bioreactor could address this challenge by being customized for all types and sizes of tissues.

Conclusion

To our knowledge, this is the only comparative study to assess the optimal perfusion decellularization protocol for rodent fasciocutaneous free flaps. A decellularization protocol of 5 days of 1% SDS solution followed by 1 day of 1% Triton X-100 and 1 day of 1x PBS was the most successful to keep the residual DNA content at a minimum while preserving the structural integrity of the tissues. The bioreactor is capable of running automated and repeatable protocols using several solutions and continuously perfusing fluid throughout the vasculature of a free flap. This compact and integrated system can decrease hands-on time and be used in the future for further recellularization of scaffolds to bioengineer complex soft tissue replacement without donor-site morbidity.

Conflict of Interest
None declared.

References

1 Hallock GG. Complications of 100 consecutive local fasciocutaneous flaps. Plast Reconstr Surg 1991;88(02):264–268
2 Buchanan PJ, Kung TA, Cederna PS. Evidence-based medicine: wound closure. Plast Reconstr Surg 2016;138(3, Suppl): 257S–270S
3 Mirzabeigi MN, Wilson AJ, Fischer JP, et al. Predicting and managing donor-site wound complications in abdominally based free flap breast reconstruction: improved outcomes with early reoperative closure. Plast Reconstr Surg 2015;135(01):14–23
4 Hallock GG. Complications of the free-flap donor site from a community hospital perspective. J Reconstr Microsurg 1991;7 (04):331–334
5 Siemionow M, Ortak T, Izycki D, et al. Induction of tolerance in composite-tissue allografts. Transplantation 2002;74(09): 1211–1217
6 Kueckelhaus M, Fischer S, Seyda M, et al. Vascularized composite allotransplantation: current standards and novel approaches to prevent acute rejection and chronic allograft deterioration. Transpl Int 2016;29(06):655–662
7 Ott HC, Clippinger B, Conrad C, et al. Regeneration and orthotopic transplantation of a bioartificial lung. Nat Med 2010;16(08): 927–933
8 Ott HC, Matthiesen TS, Goh SK, et al. Perfusion-decellularized matrix: using nature's platform to engineer a bioartificial heart. Nat Med 2008;14(02):213–221
9 Song JJ, Guyette JP, Gilpin SE, Gonzalez G, Vacanti JP, Ott HC. Regeneration and experimental orthotopic transplantation of a bioengineered kidney. Nat Med 2013;19(05):646–651
10 Crapo PM, Gilbert TW, Badylak SF. An overview of tissue and whole organ decellularization processes. Biomaterials 2011;32 (12):3233–3243
11 Scarritt ME, Pashos NC, Bunnell BA. A review of cellularization strategies for tissue engineering of whole organs. Front Bioeng Biotechnol 2015;3(MAR):43
12 Folkman J, Hochberg M. Self-regulation of growth in three dimensions. J Exp Med 1973;138(04):745–753
13 Poornejad N, Buckmiller E, Schaumann L, et al. Re-epithelialization of whole porcine kidneys with renal epithelial cells. J Tissue Eng 2017;8:2041731417718809
14 Robertson MJ, Dries-Devlin JL, Kren SM, Burchfield JS, Taylor DA. Optimizing recellularization of whole decellularized heart extracellular matrix. PLoS One 2014;9(02):e90406

15 Lu TY, Lin B, Kim J, et al. Repopulation of decellularized mouse heart with human induced pluripotent stem cell-derived cardiovascular progenitor cells. Nat Commun 2013;4:2307
16 Montserrat N, Garreta E, Izpisua Belmonte JC. Regenerative strategies for kidney engineering. FEBS J 2016;283(18): 3303–3324
17 Gilpin SE, Ren X, Okamoto T, et al. Enhanced lung epithelial specification of human induced pluripotent stem cells on decellularized lung matrix. Ann Thorac Surg 2014;98(05):1721–1729, discussion 1729
18 Guyette JP, Gilpin SE, Charest JM, Tapias LF, Ren X, Ott HC. Perfusion decellularization of whole organs. Nat Protoc 2014;9 (06):1451–1468
19 Shandalov Y, Egozi D, Koffler J, et al. An engineered muscle flap for reconstruction of large soft tissue defects. Proc Natl Acad Sci U S A 2014;111(16):6010–6015
20 Jank BJ, Goverman J, Guyette JP, et al. Creation of a bioengineered skin flap scaffold with a perfusable vascular pedicle. Tissue Eng Part A 2017;23(13-14):696–707
21 Qu J, Van Hogezand RM, Zhao C, Kuo BJ, Carlsen BT. Decellularization of a fasciocutaneous flap for use as a perfusable scaffold. Ann Plast Surg 2015;75(01):112–116
22 Zhang Q, Johnson JA, Dunne LW, et al. Decellularized skin/adipose tissue flap matrix for engineering vascularized composite soft tissue flaps. Acta Biomater 2016;35:166–184
23 Giatsidis G, Guyette JP, Ott HC, Orgill DP. Development of a large-volume human-derived adipose acellular allogenic flap by perfusion decellularization. Wound Repair Regen 2018;26(02):245–250
24 Gilbert TW. Strategies for tissue and organ decellularization. J Cell Biochem 2012;113(07):2217–2222
25 Maghsoudlou P, Georgiades F, Smith H, et al. Optimization of liver decellularization maintains extracellular matrix micro-architecture and composition predisposing to effective cell seeding. PLoS One 2016;11(05):e0155324
26 Price AP, Godin LM, Domek A, et al. Automated decellularization of intact, human-sized lungs for tissue engineering. Tissue Eng Part C Methods 2015;21(01):94–103
27 Schilling BK, Lamberti KK, Snowden MJ, et al. Design and fabrication of an automatable, 3D printed perfusion device for tissue infusion and perfusion engineering. Tissue Eng Part A 2020;26(5-6):253–264
28 Casal D, Pais D, Iria I, et al. A model of free tissue transfer: the rat epigastric free flap. J Vis Exp 2017;(119):55281
29 Gerli MFM, Guyette JP, Evangelista-Leite D, Ghoshhajra BB, Ott HC. Perfusion decellularization of a human limb: a novel platform for composite tissue engineering and reconstructive surgery. PLoS One 2018;13(01):e0191497
30 Bae H, Puranik AS, Gauvin R, et al. Building vascular networks. Sci Transl Med 2012;4(160):160ps23
31 Seetapun D, Ross JJ. Eliminating the organ transplant waiting list: the future with perfusion decellularized organs. Surgery 2017; 161(06):1474–1478
32 Kim IH, Ko IK, Atala A, Yoo JJ. Whole kidney engineering for clinical translation. Curr Opin Organ Transplant 2015;20(02):165–170
33 Fu RH, Wang YC, Liu SP, et al. Decellularization and recellularization technologies in tissue engineering. Cell Transplant 2014;23 (4-5):621–630
34 Cui H, Chai Y, Yu Y. Progress in developing decellularized bioscaffolds for enhancing skin construction. J Biomed Mater Res A 2019; 107(08):1849–1859
35 Naik A, Griffin MF, Szarko M, Butler PE. Optimizing the decellularization process of human maxillofacial muscles for facial reconstruction using a detergent-only approach. J Tissue Eng Regen Med 2019;13(09):1571–1580
36 Naik A, Griffin M, Szarko M, Butler PE. Optimizing the decellularization process of an upper limb skeletal muscle; implications for muscle tissue engineering. Artif Organs 2020;44(02):178–183
37 Duisit J, Maistriaux L, Bertheuil N, Lellouch AG. Engineering vascularized composite tissues by perfusion decellularization/recellularization: review. Curr Transplant Rep 2021;8(02): 44–56
38 Bengur FB, Solari MG. Extracorporeal perfusion of vascularized composite tissues: the bridging role of an emerging technology in reconstructive microsurgery. Plast Reconstr Surg Glob Open 2022;10(10):e4578
39 Egro FM, Schilling BK, Fisher JD, et al. The future of microsurgery: vascularized composite allotransplantation and engineering vascularized tissue. J Hand Microsurg 2022 (e-pub ahead of print). Doi: 10.1055/s-0042-1757182
40 Singer VL, Jones LJ, Yue ST, Haugland RP. Characterization of PicoGreen reagent and development of a fluorescence-based solution assay for double-stranded DNA quantitation. Anal Biochem 1997;249(02):228–238
41 Holden MJ, Haynes RJ, Rabb SA, Satija N, Yang K, Blasic JR Jr. Factors affecting quantification of total DNA by UV spectroscopy and PicoGreen fluorescence. J Agric Food Chem 2009;57(16): 7221–7226
42 Lupon E, Lellouch AG, Acun A, et al. Engineering vascularized composite allografts using natural scaffolds: a systematic review. Tissue Eng Part B Rev 2022;28(03):677–693
43 Jank BJ, Xiong L, Moser PT, et al. Engineered composite tissue as a bioartificial limb graft. Biomaterials 2015;61:246–256
44 Duisit J, Maistriaux L, Taddeo A, et al. Bioengineering a human face graft: the matrix of identity. Ann Surg 2017;266(05):754–764
45 Duisit J, Amiel H, Wüthrich T, et al. Perfusion-decellularization of human ear grafts enables ECM-based scaffolds for auricular vascularized composite tissue engineering. Acta Biomater 2018; 73:339–354